

MFN 05-116  
Enclosure 1

**ENCLOSURE 1**

**MFN 05-116**

**DCD Appendix 3L,  
“Reactor Internals Flow Induced Vibration Program”**

Conditional Release – pending closure of design verifications

## **Appendix 3L. Reactor Internals Flow Induced Vibration Program**

### **3L.1 Introduction**

A flow-induced vibration (FIV) testing program of the reactor internal components of the ESBWR prototype plant is to be completed to demonstrate that the ESBWR internals design can safely withstand expected FIV forces for reactor operating conditions up to and including 100% power and core flow. This program includes an initial evaluation phase that has the objective of demonstrating that the reactor internals are not subject to FIV issues that can lead to failures due to material fatigue, or fretting and wear issues. Throughout this part of the program, the emphasis will be placed on demonstrating that the reactor components will safely operate for the design life of the plant. The second phase of the program is focused on preparing and performing the startup test program that demonstrates through instrumentation and inspection that no FIV problems exist. This part of the program meets the requirements of Regulatory Guide 1.20 with the exception of those requirements related to preoperational testing, that cannot be performed for a natural circulation plant.

### **3L.2 Reactor Internal Components FIV Evaluation**

The ESBWR reactor internals are part of an evolutionary BWR design, but fundamentally the components and operation of the reactor vessel and internals are very similar to past BWRs. To a large extent the ESBWR design of the components relies heavily on the prior design of internals in operating plants to assure that new vibration issues are not introduced. Also, to assure that the flow of steam or water in the reactor vessel is comparable to prior reactors, efforts were made to maintain traditional spacing and dimensional relationships of components. A unique feature of the ESBWR, with respect to FIV, is the fact that it is a natural circulation plant where no recirculation motors exist that would create pressure pulses from the pump vanes that would travel into the reactor vessel. The pump vane passing frequency, that is variable with flow, typically has a maximum frequency of 120 Hz at full reactor flow. This source of excitation has caused failures in small components inside BWR reactor vessels. For ESBWR this source of flow excitation does not exist. The design of the ESBWR reactor internals is shown in figure 5.5-3.

#### **3L.2.1 Evaluation Process – Part 1**

The first step in the evaluation process was to establish selection criteria for reactor internal components related to susceptibility to vibration. All reactor internal components were considered as potential candidates for further evaluation. Each component is evaluated against the following selection criteria:

Is the component critical to safety?

Is the component of a significantly different or new design compared to earlier BWRs?

Does the component have a history of FIV-related problems?

Is the component subjected to significantly different or new flow conditions?

Based on these criteria, the following internal component structures are considered to be candidates for additional evaluation and potential to be instrumented in the startup FIV test program:

Steam Dryer Bank Hoods and End Plates based on history of past FIV related problems (fatigue cracking between hood and endplate).

Steam Dryer Skirt based on history of past FIV-related problems (fatigue cracking between skirt and drain channels).

Steam Dryer Drain Channels based on history of FIV-related problems (fatigue cracking between skirt and drain channels).

Steam Dryer Support Ring based on history of FIV-related problems (dryer rocking) and the resulting new design features for replacement dryer designs (e.g., strengthened weld joints, castings).

Chimney partition assembly based on new design features (elongated chimney shell, partition assembly, chimney restraint), potential new flow conditions, difficulty of repair in event of failure, and limited ability to change the design due to dimensional constraints.

Chimney Head / Steam Separator assembly based on new design (flat head with beam reinforcement and elongated standpipes).

Shroud /Chimney assembly based on new design features (discrete shroud support members and the chimney connection), potential new flow conditions and difficulty of repair in event of failure.

Standby Liquid Control (SLC) internal piping based on new design and being critical to safety.

Control Rod Guide Tubes (CRGTs) based on new design features (shortened length) and potential new flow conditions.

In-Core Monitor Guide Tubes (ICMGTs) based on new design features (stabilizer ties to shroud or shroud support), potential new flow conditions and difficulty of repair in the event of failure.

In-Core Monitor Housings (ICMH) based on new design features (stabilizer ties to shroud or shroud support), potential new flow conditions and difficulty of repair in the event of failure.

Other components that are not specifically identified as candidates for the instrumentation program are basically proven by past trouble-free BWR experience and have designs and flow conditions that are similar to prior operating BWR plants.

From this list, the first priority was determined to be the chimney partition assembly. This selection was made since it was a new component where only limited operating experience was available. Also, it is a structure where the geometry of the partitions places limitations on the plate thicknesses, has a long extended length, and is subject to high velocity two-phase steam flow. From this initial selection, a test and analysis program was established and the results are discussed in section 3. For this case, testing was required since no prior relevant test data was available for this component.

The steam dryer was established as the second priority. An initial analysis program was started to study the acoustic and flow effects of the ESBWR configuration in comparison to the ABWR steam dryer design. It was determined that the increase in the size of the steam dryer support ring and skirt design, and the increase in steam velocity did not have any adverse effects on the steam dryer structural integrity. At the time of the initial assessment, it was also recognized that the evaluation of BWR operating plant dryer loads was an ongoing program that would need to be ultimately factored into the ESBWR steam dryer design and evaluation effort. The progress of the generic steam dryer program is now at a stage that a meaningful effort can now be planned for the ESBWR steam dryer. The detailed program that is planned is described in section 4. As a result of the advances in the understanding of dryer vibration and differential pressure loads and steam dryer design improvements, the ESBWR will use a steam dryer design patterned after the replacement steam dryer design developed for BWR operating plants.

The next part of the evaluation phase will be to complete a more quantitative evaluation of the remaining components with the objective of documenting the existing facts regarding the individual components. This part of the evaluation will focus on the following:

1. Similarities and differences of the ESBWR component design configurations as compared to prior designs. In most cases the comparison design will be with the ABWR components.
2. A review of prior component calculations for the comparison designs, from item 1, to establish the mode shapes and natural frequencies. Estimates of the ESBWR component natural frequencies will then be determined based on this data.
3. Prior plant startup instrumentation data from the prototype ABWR plant will be reviewed to establish the magnitude and frequency of the measured vibration data, and to review the resulting calculated stress for the components that were instrumented.

4. A comparison of the flow paths and characteristics of the ESBWR design will be compared to prior BWR designs where a startup vibration test program was conducted.
5. Using the results of the above items, an assessment as to likelihood of FIV issues will be completed and documented in a supplemental report. The objective in some cases will be to conclusively demonstrate that FIV will not be an issue and that safety will not be adversely affected. In other cases, the conclusions may determine that additional evaluation or instrumentation is necessary. For these cases, no FIV issues are anticipated, and the objective is to provide additional supporting information that clearly demonstrates that FIV is not an issue.

### **3L.2.2 Evaluation Process – Part 2**

The next phase of the evaluation program will be to perform additional work to demonstrate the adequacy of components where it was determined that additional evaluations were required, and to do the next steps that are necessary for those components that are planned for instrumentation in the ESBWR startup test program. During this phase, the process as identified in paragraph 3.9.2.3 will be followed to prepare finite element analysis models per the details shown in paragraph 3L.5.5.1, establish correlation functions based on prior instrumentation data, and apply the correlation functions to the model to determine expected stress amplitude. The results of these evaluations will be documented in a supplemental report.

Because most of the reactor internal components are large durable components where there has been no history of FIV issues, no FIV issues are anticipated. Also, because it is still early in the program, there is still the opportunity to make adjustments as necessary in the component designs to make them more resistant to FIV.

## **3L.3 Chimney Partition Assembly Evaluation**

### **3L.3.1 Design and Materials**

The chimney partition assembly design consists of a bottom ring of the partition assembly that rests on and is bolted and pinned to the bottom flange of the chimney. The top ring of the partition assembly is supported against the inside of the chimney shell. The partitions are a grid of square structures, each of which encompasses 16 fuel assemblies. The partitions are to be fabricated using stainless steel plate that is full length welded at the junctions of the partitions. The stainless steel material has a 0.02% maximum carbon content to resist IGSCC. The chimney structure that houses the partition structure is cylindrical and similar to the core shroud. A sketch of the chimney and partition assembly is shown in Figure 3L-1. Since the chimney has structural characteristics similar to the shroud, this component is

considered under the generic reactor internals vibration program, and the partition assembly is considered to be the unique component that requires special vibration consideration

### **3L.3.2 Prior Operating Experience**

Prior to the ESBWR design, only one other BWR plant had operating experience with this chimney design. This was the BWR-1 Dodewaard plant, which did not have a vibration instrumentation program. For this plant, the partition size was a square configuration that encompassed four fuel assemblies within the cell, which is  $\frac{1}{4}$  the dimension of the ESBWR partitions. Also, the height was approximately  $\frac{1}{2}$  the length of the ESBWR design. The partition thickness was 3 mm (0.125 inches) as compared to 9 mm for ESBWR, and the partitions were welded together using intermittent fillet welds as compared to full-length welds for ESBWR. Although the partitions were not instrumented, the plant operated for almost 30 years without any issues related to the chimney structure. Since the design of the ESBWR chimney partitions is more robust, its operational history provides additional assurance that the ESBWR will not have FIV issues.

### **3L.3.3 Testing and Two-phase Flow Analysis**

For the ESBWR, the chimney lattice partition assembly constitutes a structure that needs to have a unique vibration evaluation program as part of the ESBWR reactor internals. In order to assess its capability to maintain structural integrity under plant operating conditions, a flow induced vibration evaluation has been performed in which the fluctuating fluid force acting on the partition plates has been evaluated by a combination of scale tests and two-phase flow analysis.

The test scope comprised both 1/6-scale (100mm × 100mm) and 1/12-scale (50mm × 50mm) air and water two-phase flow testing of a single chimney cell. The superficial velocities of the gas and liquid components of the two-phase flow were adjusted to be consistent with ESBWR values to simulate the actual two-phase flow pattern. Different inlet flow conditions were used to investigate the influence of inlet mixing within the partition to simulate different power conditions. Pressure fluctuation was measured on the inner surface of the partition wall with pressure transducers.

The results of the scale testing were extrapolated by a two-phase flow analysis to determine the characteristics of the pressure fluctuations acting on the partition wall of a full size cell in steam-water conditions. This extrapolation included the use of a 1/12 and full scale analytical model. The resulting peak-to-peak pressure fluctuation was determined to be 15 kPa at a peak frequency of approximately 2 Hz.

A structural analysis of the chimney and partition design was then conducted using finite element methods. First, an eigenvalue analysis determined that the lowest natural frequency of the chimney structure is approximately 56 Hz. This was sufficiently greater than the predominant frequency of pressure fluctuation determined by testing (2 Hz) that a static analysis of the structure was concluded to be proper. Based on the results of that static analysis, a maximum stress of 41 MPa was calculated near the edge of the partition plate

joint. This stress value is bounded by the allowable vibration peak stress amplitude of 68.95 MPa specified in Subsection 3.9.2.3.

## **3L.4 Steam Dryer Evaluation Program**

### **3L.4.1 Steam Dryer Design and Performance**

The ESBWR steam dryer will be designed using modules of dryer vanes enclosed in a housing to make up the steam dryer assembly. The modules or subassemblies of dryer vanes, called dryer units, will be arranged in six parallel rows called banks. The dryer banks will be attached to an upper support ring, which is supported by steam dryer support brackets that are welded attachments to the RPV. The steam dryer assembly will not physically connect to the shroud head and steam separator assembly and will have no direct connection with the core support or shroud. A cylindrical skirt will attach to the upper support ring and will project downward to form a water seal around the array of steam separators. Normal operating water level will be approximately mid-height on the dryer skirt.

Wet steam from the core will flow upward from the steam separators into an inlet header, horizontally through the dryer vanes, the outlet side perforated plates, vertically in the outlet header and out into the RPV dome. Dry steam will then exit the reactor pressure vessel (RPV) through the steam outlet nozzles. Moisture (liquid) will be separated from the steam by the vane surface and the hooks attached to the vanes. The captured moisture will flow downward, under the force of gravity, to a collection trough that carries the liquid flow to drain vertical drain channels. The liquid will flow by gravity through the vertical drain channels to the lower end of the skirt where the flow will then exist below normal water level. Table 3L-1 provides a comparison between major configuration parameters of the ESBWR and an ABWR steam dryer.

During normal refueling outages, the ESBWR steam dryer will be supported from the floor of the equipment pool by the lower support ring that is located at the bottom edge of the skirt. The steam dryer will be installed and removed from the RPV by the reactor building overhead crane. A steam separator and dryer lifting device, which attaches to four steam dryer lifting rod eyes, will be used for lifting the dryer. Guide rods in the RPV will be used to aid dryer installation and removal. Upper and lower guides on the dryer assembly will be used to interface with the guide rods. The ESBWR steam dryer assembly is shown in Figure 3L-2.

### **3L.4.2 Materials and Fabrication**

Current industry practice will be applied to the materials and fabrication of the ESBWR steam dryer. The steam dryer materials are selected to be resistant to corrosion and stress corrosion cracking in the BWR steam/water environment. New industry dryers are currently constructed from wrought 300 series stainless steel and Grade CF3 stainless steel castings. Except for the dryer vane material, the maximum carbon content of the wrought stainless steel will be limited to 0.02% and the maximum hardness of wrought 300 series stainless

steel will be limited to Rockwell B92. Fabrication process controls are applied to minimize the degradation of material properties by forming, cold working, etc. Susceptibility to stress corrosion cracking will be avoided by careful control of the solution heat treatment, sensitization testing and testing for intergranular attack (IGA).

### 3L4.3 Load Combinations

Design loads for the steam dryer will be based on evaluation of the ASME load combinations provided in Table 3.9-2 except that the load definitions that pertain to the steam dryer are modified as shown in Table 3L-2. These load combinations consist of dryer deadweight loads, static and fluctuating differential pressure loads (including turbulent and acoustic sources), seismic, thermal, and transient acoustic and fluid impact loads.

### 3L4.4 Fluid Loads on the Dryer

During normal operation, the dryer experiences a static differential pressure loading across the dryer plates resulting from the pressure drop of the steam flow across the vane banks. The dryer also experiences fluctuating pressure loads resulting from turbulent flow across the dryer and acoustic sources in the vessel and main steamlines. During transient and accident events, the dryer may also experience acoustic and flow impact loads that result from system actions (e.g., turbine stop valve closure) or from the system response (e.g., the two-phase level swell following a main steamline break).

Of particular interest are the fluctuating pressure loads that act on the dryer during normal operation that has led to fatigue damage in previous dryer designs. Scale model testing has identified the likely sources of fluctuating pressure loading acting on the steam dryer. The results of this testing showed that the fluctuating pressure load frequency spectrum can be divided into four regions based on the postulated source of the loading:

**0-10 Hz:** The pressure loads in this frequency range are dominated by the fundamental main steamline piping acoustics. The source of these pressure loads is believed to be turbulence in the main steamline or vortex shedding in steam dome.

**10-30 Hz:** The source of the pressure loads in this frequency range is postulated to be a stationary vortex on the outer hood of the steam dryer adjacent to the vessel outlet nozzles. The frequency characteristics of this pressure loading may be governed by harmonics of the main steamline acoustics.

**>30 Hz:** The lowest steam plenum acoustic modes are located in this frequency range. The dominant excitation is due to broadband turbulent sources located in main steamlines but the acoustic modes may also be excited by sources in the vessel. The plenum acoustic modes have a very high amplification effect on pressure oscillations in this frequency range. The lower frequency vessel acoustic modes exhibit the most significant response to the turbulent excitation present in the system. Higher frequency vessel acoustics exist but are not significantly excited except as discussed below.



**120-200 Hz:** Strong narrow band pressure loads in this frequency range are caused by acoustic resonances in safety and relief valve branch lines attached to the main steamlines. Higher frequency steam plenum acoustic modes can be excited if the vessel is acoustically coupled to the branch line. The ESBWR SRV standpipe design is intended to reduce or eliminate acoustic resonances in these branch lines.

The steam dryer acoustic load definition process consists of three primary elements: scale model testing (physical testing using an ESBWR scale model to acquire load definition data, pressure and frequency, monitored by approximately 60 transducers), acoustic finite element modeling of the reactor steam dome region to determine the natural frequencies and mode shapes of the steam volume, and a load interpolation algorithm to refine the measured fluctuating load into a fine mesh consistent with the structural finite element model nodalization in order to perform an accurate stress analysis of the dryer.

Flow induced turbulent and acoustic loads for the design of the ESBWR steam dryer will be determined from scale model testing of the dryer design and resultant acoustic modeling performed in the GE scale model testing facility located at the Vallecitos Nuclear Center in Sunol, California. The scale model test apparatus models the outside surface of the steam dryer above the vessel water level, the vessel steam dome region, and the main steamline piping to the turbine inlet, including major branch lines (e.g., SRV standpipes, turbine bypass piping). The testing is performed in ambient air conditions. Because the fluctuating pressure loads are primarily acoustic in nature, the test results are scaled to reactor conditions while preserving an equivalent Mach number between the model and the plant. GE has recently completed a power ascension test program with an instrumented BWR 3 steam dryer. The scale model test has been benchmarked against the plant data acquired from this instrumented dryer and confirms the capability of the GE scale model test methodology to predict the steam dryer acoustic load definitions.

The acoustic finite element model models the steam dryer and reactor steam dome cavity. This model is used to predict the acoustic mode shapes of the cavity and provides the framework for the load interpolation algorithm.

The load interpolation algorithm is used to provide a fine mesh load definition for input to the dynamic structural analysis. The algorithm uses the acoustic normal modes of the RPV steam plenum as a basis to describe the domain of interest. The algorithm uses the test measurements taken from the approximately 60 transducer locations on the scale model test and the acoustic finite element model to develop a fine-mesh array of pressure time histories that are consistent with the structural finite element model nodalization.

#### **3L.4.4 Structural Evaluation**

A finite element analysis (FEA) will be performed to confirm that the ESBWR steam dryer is structurally acceptable for operation. The FEA will use the scale model test loads as input. The finite element analysis will be performed using a whole dryer analysis model of the ESBWR steam dryer to determine the most highly stressed locations. The FEA consists of time history dynamic analyses for the load combinations identified in Table 3.9-2. If

required, locations of high stress identified in the whole dryer analysis will be further evaluated using solid finite element models to more accurately predict stresses at these locations. The analysis will also confirm that the RPV dryer support lugs will accommodate the predicted dryer loads under normal operation and transient and accident conditions. (also see 3.L.5.5.1.5)

The structural evaluation of the ESBWR steam dryer design will be presented during the certification phase.

### **3L.4.6 Instrumentation and Startup Testing**

The ESBWR steam dryer will be instrumented with temporary vibration sensors to obtain flow induced vibration data during power operation. The primary function of this vibration measurement program is to confirm the actual pressure loading on the dryer during power operation is consistent with the pressure loading assumed in the structural fatigue evaluation and to verify that the new steam dryer can adequately withstand flow induced vibration forces for extended period as designed. The detailed objectives are as follows:

- a. Determine the dryer as-built modal parameters: This will be achieved by impact (hammer) testing the dryer components. The results will yield natural frequencies, mode shapes and damping of the dryer components for the as-built dryer. These results will be used to verify portions of the analytical model of the dryer.
- b. Confirm the pressure loading: In order to confirm the pressure loading on the dryer due to turbulence, acoustics and other sources, dynamic pressure sensors will be installed on the dryer. These measurements will provide the actual pressure loading on the dryer under various operating conditions.
- c. Verify the new dryer design: Based on past knowledge gained from different dryers, as well as information gleaned from analysis of the new dryer design, selected areas of the dryer will be instrumented with strain gages and accelerometers to measure vibratory stresses and displacements on the dryer during power operation. The measured strain values will be compared with the allowable values (acceptance criteria) obtained from the analytical model to confirm that the dryer alternating stresses are within allowable limits.

The steam dryer vibration sensors will consist of strain gauges, accelerometers and dynamic pressure sensors, appropriate for the application and environment. A typical list of vibration sensors with their model numbers is provided in Table 3L-3. The selection and total number of sensors will be based on past experience of similar tests conducted on other BWR steam dryers. These sensors will be specifically designed to withstand the reactor environment.

Each of the sensors will be pressure tested in an autoclave prior to assembly and installation on the dryer. An uncertainty analysis will be performed to calculate the expected uncertainty in the measurements.

Prior to initial plant start-up, strain gauges will be resistance spot-welded directly to the dryer surface. Accelerometers will be tack welded to pads that are permanently welded to the dryer surface. Surface mounted pressure sensors will be welded underneath a specially designed dome cover plate to minimize flow disturbances that may affect the measurement. The dome cover plate with the pressure transducer will be welded to an annular pad that is welded permanently to the dryer surface. All the sensor conduits will be routed along a mast on the top of the dryer and fed through the RPV instrument nozzle flange to bring the sensor leads out of the pressure boundary. Sensor leads will be routed through the drywell to the data acquisition area outside the primary containment.

Pressure transducers and accelerometers are typically piezoelectric devices, requiring remote charge converters that will be located in junction boxes inside the drywell. The data acquisition system will consist of strain gauges, pressure transducers and accelerometer signal conditioning electronics, a multi-channel data analyzer and a data recorder. The vibration data from all sensors will be recorded on magnetic or optical media for post processing and data archival. The strain gauges, accelerometer and pressure transducers will be field calibrated prior to data collection and analysis. The temporary vibration sensors will be removed after the first outage.

During power ascension, the steam dryer instrumentation (strain gages, accelerometers and dynamic pressure transducers) will be monitored against established limits to assure the structural integrity of the dryer is maintained. If resonant frequencies are identified and increase above the predetermined criteria, power ascension will stop. The acceptability of the dryer for the measured loading will be evaluated and revised operating limits defined as required.

Future steam dryer inspections will be in accordance with GE SIL 644 Revision 1 and BWRVIP-139.

### **3L.5 Startup Test Program**

This section summarizes the program for preparing and performing the startup FIV testing including the methods and analysis that will be performed when the startup test data is available. This section will assume that the initial selection of components identified in section 3L.2.1 will be part of the analysis and instrumentation associated with the startup testing program.

#### **3L.5.1 Component Selections**

The components that are selected for instrumentation are determined from the initial evaluation phase as discussed in section 3L.2.1. Many different sensors of four different types are utilized to measure vibration related data on several different reactor internal component structures.

### **3L.5.2 Sensor Locations**

Having determined the components to instrument during the test, sensor locations on those structures are determined based upon the analytically predicted mode shapes for each structure or, in some cases, based upon the location of past FIV-related failures. Strain gages, accelerometers and linear variable differential transformer (LVDT) type relative displacement sensors are used for monitoring vibration levels. Strain gages measure local strain from which local stress can be calculated. Based on knowledge of the natural mode shapes of the structure, peak stresses at other locations on the structure are determined from these data. Accelerometers (with double integration of the output signal) and LVDTs provide measurements of local structural displacement. This information, together with knowledge of the natural mode shapes of the structure, allows the peak stresses to be calculated at other locations. Pressure sensors are also utilized at various locations in the vessel. These are not used to measure structural vibration directly, but rather to measure the pressure variation that is often a forcing function that causes the structural vibration. These pressure sensor data are very useful for determining the source of any excessive vibration amplitudes, if they are to occur during testing. Typical sensor types and potential locations are listed in Table 3L-4.

### **3L.5.3 Test Conditions**

Test conditions are selected early in the FIV test program to consider a variety of steady-state and transient operating conditions that could be expected to occur during the life of the plant.

Reactor pressure vessel (RPV) internals vibration at steady-state conditions is more important than transient conditions for evaluating the structural integrity of components. This is because steady-state normal operating conditions can exist for long periods of time, allowing a very large number of vibration cycles to accumulate. Flow-induced vibration caused by transient operating conditions is far less influential because of the relatively low number of vibration cycles that will occur over the lifetime of the plant. The purpose in including transient test conditions is to confirm that extremely high stresses do not occur during transients. This check is accomplished during the actual startup transient tests by the vibration engineers monitoring the test equipment. Transient stress levels near the allowable limit would be easily and immediately detected by the vibration engineers. No such high stress levels are expected to occur during the ESBWR prototype plant FIV transient tests. Therefore, for the purposes of confirming the structural capability of the internals, steady-state test conditions are the most important conditions to evaluate.

Total volumetric core flow rate is also an important parameter that affects the vibration magnitude of the internals. Vibration amplitude generally increases as the volumetric flow rate increases.

### **3L.5.4 Data Reduction Methods**

Basically, two types of data reduction are performed: (1) time history analyses and (2) spectrum analyses. In either data reduction method, the measured peak-to-peak (p-p) value of each sensor signal is compared to the allowable p-p value. Even though both time history and spectrum analyses are performed for each selected sensor and test condition, the results from only one data reduction method are used for comparison to the allowable values. The selection of the method is dependent on the analysis method used for data evaluation. The different methods of data evaluation are described in detail in Section 3L.5.5. Briefly, Method I is used for components that have many closely spaced natural vibration modes and utilizes the strain energy weighting method applied to all modes over the frequency range of interest. This method has previously been applied to the In-core Monitor (ICM) housings, shroud, top guide, and steam dryer skirt and support ring. Method II is similar to Method I, except that it is applied to two frequency bands, 0-100 Hz and 100-200 Hz. This method has previously been applied to the steam dryer drain channels and hood. Method III is used for components that have relatively few, distinct dominant natural modes that are matched to the analytical modes. This method has previously been applied to the in-core guide tubes. Table 3L-5 describes the method of data reduction that is applicable to each component.

#### **3L.5.4.1 Time History Analysis**

The time history method uses the analyzer's time capture mode of operation. The time capture is performed for a period of several minutes for all the selected sensors and test conditions. The frequency bandwidth for the time capture is chosen to accommodate 0-200 Hz as a minimum for most channels.

For comparison to the allowable vibration amplitude, the p-p over specified bandwidths needs to be obtained for sensors in specific components. The bandwidths used for p-p measurements for various components are shown in Table 3L-5. There are four bandwidths for time history p-p measurement: 0-200 Hz, 0-100 Hz, 100-200 Hz and 0-1600 Hz. The 0-1600 Hz is used only for the accelerometer for the purpose of detecting impacts. The other three bandwidths are used for normal vibrations.

For the 0-200 Hz bandwidth, the maximum p-p values over several minutes of data for selected sensors and test conditions are obtained directly from the time capture. Specification of the bandwidth for time capture (0-200 Hz) automatically results in a low-pass filtered signal.

In order to obtain the maximum p-p in the 0-100 Hz range, the histogram operation is employed on the time capture traces. When the bandwidth (0-100 Hz) is specified in the histogram operation, the signal is automatically low-pass filtered in the specified frequency range. The histogram measurement shows how the amplitude of the input signal is distributed between its maximum and minimum values. The horizontal axis is the amplitude axis and usually the center of the horizontal axis is the zero point with positive and negative amplitudes on either side of the zero. The vertical axis is the number of counts or the number of times a particular amplitude value occurs in a time-history. From the histogram, the

maximum positive and maximum negative values in a time history can be obtained, from which the maximum p-p of the time history can be obtained.

For the 100-200 Hz bandwidth range, the time captured traces are filtered in the 100-200 Hz range and the p-p is obtained over a period of several minutes. The filtered time history between 100 and 200 Hz is scanned to obtain maximum and minimum values to get p-p values.

For the 0-1600 Hz range for accelerometers, the time history signal is examined for the presence of any impacts.

### **3L.5.4.2 Frequency Analysis**

The spectrum shows the signal in the frequency domain. There are several different types of spectra. The linear spectrum is the Fourier transform of the time history signal. The auto power spectrum is the magnitude squared of the linear spectrum, which is computed by multiplying the Fourier transform of the signal by its complex conjugate. This spectrum contains magnitude information only. The spectra generated for ESBWR data reduction are auto power spectra. The spectra for selected sensors and test conditions are obtained from the captured time history described previously.

Signal averaging is used to obtain better statistical properties. It is possible to select the number of averages and the type of averaging. There are three types of averaging:

Stable (normal)

Exponential

Peak Hold

The averaging method used for ESBWR is “Peak Hold”, which compares the current spectral value of each individual frequency during the analysis interval to the last spectral value and holds the larger of the two. The resultant spectrum is a composite spectrum which envelopes the spectrums of all analysis intervals. The parameters used in the spectrum generation are described in Table 3L-6.

In order to obtain greater accuracy on amplitude of the frequency spectrum, a flat top window is selected.

From the spectrum, the dominant frequencies of vibration and their root mean square (RMS) magnitudes can be identified. The frequency is in the horizontal axis and the RMS magnitude is in the vertical axis. The p-p value of vibration at each dominant frequency is obtained by multiplying the RMS value (from the peak hold spectrum) by a factor of 6. This factor is obtained from many years of reactor experience and is a conservative estimate of the p-p value. This p-p value is then used to compute the stress at the sensor location and the maximum stress in the structure.

## **3L.5.5 Data Evaluation Methods**

This section describes the methods used to evaluate the reduced test data for the purpose of determining whether maximum stress levels are below the maximum allowable fatigue stress limits for the materials. A significant portion of this evaluation lies in the determination of the natural vibration modes of the instrumented components as determined using finite element models. Section 3L.5.5.1 describes the finite element models used in this process. Section 3L.5.5.2 describes the steps involved in determining the maximum stress amplitudes from the reduced data.

### **3L.5.5.1 Finite Element Models**

Dynamic analytical finite-element models are developed for the following ESBWR prototype plant reactor internal components:

- Control Rod Guide Tubes and Control Rod Drive Housings

- In-Core Monitor Guide Tubes and Housings

- Chimney Head and Steam Separators

- Shroud and Chimney

- Steam Dryer

- Standby Liquid Control Line

The dynamic analytical finite-element models are used to predict the natural vibration frequency, modal displacement, and modal strain and stress for each of the dominant vibration response modes. Descriptions of the finite-element models are given in the following sections.

#### **3L.5.5.1.1 Control Rod Drive Guide Tubes and Housings**

A dynamic finite element model of the control rod (CR) guide tube and CR drive housing assembly is developed using the ANSYS computer code [Ref. 5-1]. The natural vibration frequency for each of the CR guide tube and CRD housing assemblies will be different due to the difference in the housing and stub tube length. During the flow-induced vibration (FIV) preoperational test, a number of guide tube assemblies are instrumented. These guide tube assemblies are modeled separately.

Three-dimensional beam elements are used to model each of the components. At each nodal point of the beam elements, six degrees of freedom (DOF) are assumed: three translations and three rotations. The applied boundary conditions and constraints are: (1) the two lateral translational DOFs are fixed at the top of the guide tube which is at the core plate elevation; (2) all six DOFs are fixed at the lower end of the stub tube, which is welded to the vessel bottom head; and (3) the interface between the guide tube and housing is assumed to be a pinned connection (i.e., only the three translational DOFs are constrained).

The masses of the CR guide tube, CRD housing, and stub tube are lumped at the nodal points. The lumped masses include both the structural mass and the water mass inside the guide tube and housing, and the displaced water outside of the guide tube, housing, and stub tube. These added water masses are used to account for the effects of water on the guide tube, housing, and stub tube assembly vibration responses. The stiffness of the CR guide tube and CRD housing is equal to those of the guide tube and housing only. The effects of the control rod within the tube and the fuel assembly above the core plate are neglected.

### **3L.5.5.1.2 In-Core Monitor Guide Tubes and Housings**

In the ESBWR prototype plant reactor, there are 76 in-core monitor (ICM) guide tube and housing assemblies. The bottom of each housing is welded to the stub tube, and the upper end of each guide tube is supported at the core plate. All 76 guide tubes are tied together via stabilizers which are attached to the shroud or shroud support. To accurately predict the vibration characteristic of the ICM guide tube and housing assembly, a coupled dynamic finite element model of the entire ICM guide tube and housing forest was developed using the ANSYS computer code [Ref. 5-1].

In the ICM guide tube forest model, all of the 76 guide tubes/housings and the stabilizer grid is modeled as 3-D prismatic beams. The guide tubes are assumed to be simply supported at the core plate elevation and with free vertical movement. The housings are modeled as being fixed at the weld to the stub tube location. The guide tubes are modeled as being tied together by the stabilizer grid as continuous structural members. This continuous interface representation is more accurate than either the fixed or the simply supported, idealized assumption because the flexibility of the stabilizer members is accounted for in the continuous representation. The stabilizer grids are attached to the shroud or shroud support at selected locations. The attachment points are modeled as being pinned along the stabilizer bar direction.

The masses of the ICM guide tube/housing and stabilizer bars are lumped at the nodal points. The lumped masses include the structural mass, the water mass inside the guide tube and housing, and the displaced water mass outside of the guide tube and housing. The stiffnesses of the guide tube and housing are equal to those of the guide tube and housing only; the effects of the interior components are not considered.

Because of the large number of ICM guide tube/housing assemblies that are coupled together by the stabilizer network and with different housing lengths, there are a large number of closely spaced natural frequencies. Listing all the extracted natural frequencies would not be informative nor is it necessary. As far as the mode shapes are concerned, they generally show a small region of the ICM guide tube/housing forest undergoing large deformation, while other regions are quiescent for a typical vibration mode shape. For a given mode being excited, the region undergoing large deformation would be the region with high stress.



#### **3L.5.5.1.4 Shroud and Chimney**

In order to determine the shroud vibration frequencies and mode shapes, an axisymmetric shell model was developed using the ANSYS computer code [Ref. 5-1]. The detailed shell model consists of both the reactor pressure vessel (RPV), chimney, chimney support, and shroud such that the hydrodynamic interaction effects between the components are accounted for. In this model, each nodal point has four degrees of freedom, namely: (1) radial displacement; (2) tangential displacement; (3) vertical displacement; and (4) meridian rotation. This shell model is applicable only to the axisymmetric finite element analysis of the shroud and vessel. Responses calculated from this model, other than that of the shroud, shall not be construed as being representative of other reactor components.

The following assumptions are made in generating the axisymmetric shell model:

Discrete components move in unison for guide tubes, steam separators, standpipes, and control rod drive housings and guide tubes.

Masses are lumped at the nodal points. Rotational inertias of the masses are neglected.

Stiffnesses of control rods, control rod drives, steam dryers, and incore housings are neglected.

Top guide beam and core plate are assumed to have zero rotational stiffness.

Masses of CRD housings below the vessel are lumped to the bottom head.

Equivalent shells are used to model the mass and stiffness characteristics of the guide tubes, steam separators, and standpipes such that they match the frequencies obtained from a horizontal beam model.

Diagonal hydrodynamic mass terms are selected such that the beam mode frequencies of the shell model agree with those from the beam model.

The RPV, chimney and shroud are modeled as thin shell elements. Discrete components such as guide tubes are modeled as equivalent thin shell elements. The shell element data are defined in terms of thickness, mass density, modulus of elasticity, and Poisson's ratio for the appropriate material and temperature.

The natural frequencies and mode shapes of the shroud shell model are given in terms of two parameters, termed "n" and "m". The "n" parameter refers to the number of circumferential waves, while the "m" parameter refers to the number of axial half-waves. Thus, for beam types of 1 vibration,  $n=1$ .

#### **3L.5.5.1.5 Steam Dryer**

The design of the steam dryer assembly for the ESBWR prototype plant is somewhat different from the past BWR designs. Specifically, the major differences are in: (1) the skirt

and support ring diameters; (2) the annulus size between the skirt and reactor pressure vessel; (3) the flow path between the dryer banks and the vessel head; and (4) the design details of the dryer skirt, drain channels and hoods. In addition, the total steam flow rate of the ESBWR prototype plant is different from past designs. These differences warrant a detailed vibration analysis and test monitoring to assure the adequacy of the new design to withstand the flow-induced vibration.

In the ESBWR prototype plant FIV test program of the dryer assembly, accelerometers and strain gages are located directly on the skirt, drain channels, support ring and hoods. In addition, pressure sensors are used to measure the pressure differentials between the inside and outside of the dryer hood and dryer skirt. The differential pressure fluctuation across the dryer hoods is the primary forcing function causing vibration of the upper part of the dryer structure. The differential pressure fluctuation across the dryer skirt is the primary forcing function causing the vibration of the steam dryer skirt.

A dynamic finite element model of the dryer assembly is developed using the ANSYS computer code [Ref. 5-1]. Due to the complicated geometry and the large size of the analytical model, major components may be modeled with coarse meshes such that their dynamic contributions are accounted for in the whole dryer assembly vibration responses. Separate refined dynamic finite element models of the major components are then developed to provide a high resolution of the component's response calculation.

The structural material properties and density for the dryer components at temperature are used in the model. The effect of the water on the dynamic responses is accounted for by using a direct lumped mass input. These added mass inputs include the submerged portions of the dryer skirt, drain channels, and the lower support ring.

Prior analytical models have predicted that the vibration modes are very closely spaced.

#### **3L.5.5.1.6 Standby Liquid Control Lines**

In the ESBWR prototype plant reactor, there are two standby liquid control pipes that enter the reactor vessel and are routed to the shroud. To accurately predict the vibration characteristic of the standby liquid control line, a dynamic finite element model of the entire line is developed using the ANSYS computer code [Ref. 5-1]. In the model the ends of the line are fixed anchor points since the lines are welded at the vessel nozzle and the shroud attachment points.

#### **3L.5.5.2 Stress Evaluation**

Maximum stress amplitude values for evaluation against allowable limits are determined from the test data and finite element models using one of three different evaluation methods. The method used for a particular component depends on the complexity of that component's vibration characteristics. All three methods yield conservatively high predictions of the maximum stress anywhere on the structure. These conservatively high stress predictions are compared against conservatively low acceptance criteria to assure that none of the components is experiencing high stress vibrations that might cause fatigue failures. Table

3L-7 lists the methods that are used for each instrumented component for the ESBWR prototype plant FIV test program.

Method I is used for components that have many closely spaced vibration frequencies and/or closely spaced natural vibration modes distributed over a relatively narrow frequency range. The method utilizes a strain energy weighting method applied to all modes over the entire frequency range. It is applied by determining the maximum peak-to-peak (p-p) amplitude from an unfiltered time history segment. This maximum value is multiplied by a combined shape factor (derived from the strain energy weighting method) and stress concentration factors to yield the maximum stress value that could be expected to be found anywhere on the structure. This value is then compared against the acceptable fatigue limit stress amplitude for the material [68.9 MPa (10,000 psi)].

Method II is used for components that have many closely spaced vibration frequencies and/or closely spaced natural vibration modes that are unevenly distributed over several frequency ranges. The method is very similar to Method I, except that it is applied over several separate frequency bands. The maximum stress amplitude values for each frequency band are then added together absolutely to yield a conservatively high value for the overall maximum stress amplitude that could be found anywhere on the structure. This value is compared to the same [68.9 MPa (10,000 psi)] limit for the material.

Method III is used for components that have relatively few, distinct dominant natural modes that can be easily identified and matched to the modes predicted by the finite element models. This method utilizes a mode shape factor for each vibration mode that relates the stress at the sensor location to the stress at the maximum stress location for that mode. Appropriate stress concentration factors are also considered in this process. Response spectra are generated from the sensor output, from which the equivalent maximum p-p strain amplitude for each mode can be determined. The mode shape and stress concentration factors are applied mode by mode to determine the maximum stress amplitude associated with each mode. Then the maximum stress amplitudes from each of the modes are added together absolutely to yield a conservatively high maximum overall stress amplitude for the structure. This value is compared to the same [68.9 MPa (10,000 psi)] limits allowed for the material.

All three methods have identical initial steps to obtain mode shape factors for each natural mode. The first five steps for all three methods are as follows (Note: The evaluation method described here relates to strain gages. Similar steps are used for accelerometers used in their displacement mode and for LVDTs.):

- (1) The dynamic finite element model of each instrumented component is used to predict the natural vibration modal displacement, frequency and stress for each vibration response mode. Specifically, the computer model provides the following results for each mode:

$\omega_i$  = Natural frequency for vibration mode i

$\{\phi\}_i$  = Mass normalized displacement mode shape for vibration mode i.

(Normalized such that the generalized mass,  $\{\phi\}_i^T [M] \{\phi\}_i$ , is unity, where  $[M]$  is the mass matrix.)

$\{\sigma\}_i$  = Normalized stress distribution for vibration mode  $i$ .  
(The stress corresponding to the mass normalized mode shape,  $\{\phi\}_i$ )

The theory and methods for calculation of these parameters may be found in any good text book on the subject of basic vibration analysis, such as “Elements of Vibration Analysis”, by Leonard Meirovitch, McGraw Hill Book Co., 1975.

- (2) For each vibration mode, stress concentration factors are applied at weld locations and regions with high stress gradient. From this information, the maximum stress intensity location and value is determined for each vibration mode.

$$\sigma_{i,\max} = \text{Max}\{SCF_i \cdot \sigma_i\} \text{ considered over the entire structure}$$

where

$SCF_i$  = Stress concentration factor at some location

$\sigma_i$  = Normalized stress intensity at the same location

$\sigma_{i,\max}$  = Normalized maximum stress intensity for mode  $i$

- (3) From the stress distribution of Step 1, a mode shape factor is derived relating the stress at the sensor to the stress at the maximum stress location as determined in Step 2:

$$MSF_i = \frac{\sigma_i(\text{at maximum stress intensity location})}{\sigma_{i,\text{sensor}}}$$

where

$MSF_i$  = Mode shape factor

$\sigma_{i,\text{sensor}}$  = Normalized stress at sensor location for vibration mode  $i$

- (4) The mode shape factor from Step 3 and the maximum allowable stress amplitude for the material [68.9 MPa (10,000 psi)] are used to determine the maximum allowable stress value at the sensor location for each mode.

$$\sigma_{i,\text{sensor,allowed}} = \frac{68.9 \text{ MPa}}{(MSF_i) \cdot (SCF_i)}$$

where

$\sigma_{i,\text{sensor,allowed}}$  = Maximum allowed zero to peak stress amplitude at sensor location for vibration mode  $i$  (stress amplitude at sensor when maximum stress amplitude in structure is 68.9 MPa)

- (5) The allowable strain for mode  $i$  ( $\epsilon_{i,allowed}$ ) is then calculated from this maximum allowed stress amplitude at the sensor location:

$$\epsilon_{i,allowed} = \frac{\sigma_{i,sensor,allowed}}{E}$$

where

$$E = \text{Young's modulus [e.g., } 1.862 \times 10^5 \text{ MPa (} 27.0 \times 10^6 \text{ psi) at } 160^\circ\text{C]}$$

This equation is for uniaxial stress components. A similar, but more complex procedure will be used for biaxial stress structures such as the dryer skirt, drain channel and hood.

At this point, Methods I and II diverge from Method III.

### 3L.5.5.2.1 Methods I and II

The next two steps are identical for Methods I and II.

- (6) A weighting factor is determined by the strain energy method, which begins by obtaining the solution to the following equation based on the expected forcing function:

$$\{U\} = q_1 \{\phi\}_1 + q_2 \{\phi\}_2 + \dots = \sum_{i=1}^N q_i \{\phi\}_i$$

where

$\{U\}$  = A vector representing the displacement response of the structure when subjected to the expected forcing function shape. This displacement response to an input forcing function is calculated from the finite element model on the computer.

$\{\phi\}_i$  = Mass normalized mode shape for vibration mode  $i$ . Mode shapes were determined from the modal analysis of the finite element model on the computer. The modes shapes are normalized such that the generalized mass,  $\{\phi\}_i^T [M] \{\phi\}_i$ , is unity (where  $[M]$  is the mass matrix).

$q_i$  = Mode  $i$  response, dependent on load distribution. These coefficients are calculated from the previously calculated  $\{U\}$  and  $\{\phi\}_i$  using formulas derived from the generalized Fourier Theorem.

This is an application of the generalized Fourier Theorem, which establishes that a displacement function such as  $\{U\}$  can be represented by a linear sum of the eigenfunctions,  $\{\phi\}_i$ . The theory and methods for calculation of these coefficients may be found in any good text book on the subject of basic vibration analysis, such

as “Elements of Vibration Analysis”, by Leonard Meirovitch, McGraw Hill Book Co., 1975.

- (7) The strain energy contribution,  $e_i$ , for each mode is then calculated:

$$e_i = \frac{1}{2} \cdot q_i^2 \cdot \{\phi\}_i^T \cdot [K] \cdot \{\phi\}_i$$

where

[K] = The structural stiffness matrix (For a more detailed explanation of the theory and calculation methods, see any good vibration analysis textbook, such as “Elements of Vibration Analysis”, by Leonard Meirovitch, McGraw Hill Book Co., 1975.)

The next step is similar for both Methods I and II, the only difference being that Method I will include the entire frequency range into one group, while Method II will break into several frequency ranges.

- (8) Then the strain energy weighted allowable strain vibration amplitude is calculated over a given frequency range by combining the weighted strain allowable values for each mode as follows:

For

$$\omega_I < \omega_1, \omega_2, \dots, \omega_n \leq \omega_{II}$$

$$\epsilon_{II,allowed} = \frac{e_1 \cdot \epsilon_{1,allowed} + e_2 \cdot \epsilon_{2,allowed} + \dots + e_n \cdot \epsilon_{n,allowed}}{e_1 + e_2 + \dots + e_n}$$

where

$\epsilon_{II,allowed}$  = Allowable strain value between  $\omega_I$  and  $\omega_{II}$ , which includes the stress concentration factor, SCF

It should be noted that this step conservatively assumes that the peak stress of each mode occurs at the same physical location on the structure. In reality, the maximum stress locations for different modes may occur at different locations. Since the purpose of this calculation is just to confirm that the maximum stress is less than an acceptable limit, it is quite acceptable to add this conservatism. However, it should be understood that the value calculated is conservatively high, and it is not an accurate prediction of the actual stress amplitude. If a stress calculated in this manner should exceed the limit in a few situations, then a less conservative calculation can be used in those few cases.

The strain value in the above equation is the allowable strain used during the actual execution of the test. It represents the strain level at the sensor location when the maximum stress on the structure is 68.9 MPa (10,000 psi).

Step 9 is the same for both Methods I and II, except that it is applied to each of the multiple frequency ranges associated with Method II; whereas, Method I is only for one frequency range.

- (9) The combined shape factor (CSF) is derived to relate the maximum zero-to-peak strain value measured at the sensor location to the corresponding maximum zero-to-peak stress intensity value on the structure.

$$\sigma_{II,max} = \frac{\epsilon_{II,measured,max}}{\epsilon_{II,allowed}} \cdot (68.9 \text{ MPa}) = \epsilon_{II,measured,max} \cdot CSF$$

where

$$CSF = \frac{(68.9 \text{ MPa})}{\epsilon_{II,allowed}} = \text{Combined Shape Factor with the SCF included.}$$

$\sigma_{II,max}$  = Maximum zero-to-peak stress value anywhere on the structure for modes within the frequency range of  $\omega_I$  to  $\omega_{II}$ .

$\epsilon_{II,measured,max}$  = Maximum measured zero-to-peak strain (one-half of maximum measured peak-to-peak) from time history of sensor band pass filtered over the frequency range  $\omega_I$  to  $\omega_{II}$ .

This is the maximum zero-to-peak stress value anywhere on the structure as determined by Method I. For Method I, this value is compared to 68.9 MPa (10,000 psi) for determination of acceptability. One additional step remains for Method II.

- (10) The maximum stress values for each frequency band are added together absolutely to determine the overall maximum stress on the structure for comparison to the 68.9 MPa (10,000 psi) limit for the material.

$$\sigma_{MAX} = \sigma_{II,max} + \sigma_{III,max} + \dots + \sigma_{N,max}$$

where

$\sigma_{MAX}$  = Maximum overall zero-to-peak stress anywhere on structure as determined by Method II.

$\sigma_{N,max}$  = Maximum zero-to-peak stress anywhere on structure within the frequency range of  $\omega_{N-1}$  to  $\omega_N$  (N-1 frequency ranges total).

$\sigma_{MAX}$  is compared to the 68.9 MPa (10,000 psi) limit in order to determine acceptability under Method II.

It should be noted that this step conservatively assumes that the peak stress of each mode occurs at the same time. In reality, the maximum stress occurs at different times. Since the purpose of this calculation is just to confirm that the maximum stress is less than an acceptable limit, it is quite acceptable to add this conservatism. However, it should be understood that the value calculated is conservatively high, and it is not an accurate



prediction of the actual stress amplitude. If a stress calculated in this manner should exceed the limit in a few situations, then a less conservative calculation can be used in those few cases.

### 3L.5.5.2.2 Method III

Method III uses the mode shape factor (MSF) from Step 3, the stress concentration factor (SCF) and the measured strain value to determine the maximum stress amplitude anywhere on the structure for each natural mode. Picking up after Step 5 from Section 5.2:

- (6) Maximum stress in the structure is calculated from the measured strain value at the sensor location.

$$\sigma_{i,MAX} = \epsilon_{i,measured,max} \cdot E \cdot MSF_i \cdot SCF_i$$

where

$\sigma_{i,MAX}$  = Maximum zero-to-peak stress anywhere on structure for mode i.

$\epsilon_{i,measured,max}$  = Maximum zero-to-peak strain for mode i as determined from power spectrum from sensor signal.

E = Young's Modulus

$MSF_i$  = Mode Shape Factor for mode i.

$SCF_i$  = Stress Concentration Factor as applicable for maximum stress location for mode i.

- (7) The maximum stress values for each mode are added together absolutely to determine the overall maximum stress on the structure for comparison to the 68.9 MPa (10,000 psi) limit for the material.

$$\sigma_{MAX} = \sigma_{1,MAX} + \sigma_{2,MAX} + \dots + \sigma_{n,MAX}$$

where

$\sigma_{MAX}$  = Maximum overall zero-to-peak stress anywhere on structure as determined by Method III.

$\sigma_{i,MAX}$  = Maximum zero-to-peak stress anywhere on structure for mode i (n total dominant modes).

$\sigma_{MAX}$  is compared to the 68.9 MPa (10,000 psi) limit in order to determine acceptability under Method III.

It should be noted that this step conservatively assumes that the peak stress of each mode occurs at the same physical location on the structure and at the same time. In reality, the maximum stress locations for different modes may occur at different locations and at different times. Since the purpose of this calculation is just to confirm that the maximum stress is less than an acceptable limit, it is quite acceptable to add these conservatisms. However, it should be understood that the value calculated is conservatively high, and it is not an accurate prediction of the actual stress amplitude. If a stress calculated in this manner should exceed the limit in a few situations, then a less conservative calculation can be used in those few cases.

In summary, all three methods involve two significant conservatisms. These are the assumption of the maximum stresses occurring at the same location in a component and the assumption that the maximum stresses for different modes occur at the same time. Inclusion of these two significant conservatisms results in significantly higher calculated stresses.

### **3L.5.5.3 References**

- 5-1 *ANSYS Engineering Analysis System User's Manual*, G.J. DeSalvo and R.W. Gorman, Swanson Analysis Systems, Inc., Houston, PA, Revision 4.4a, May 1989.
- 5-2 *Elements of Vibration Analysis*, Leonard Meirovitch, McGraw Hill Book Co., 1975.

Table 3L-1  
Comparison of Major Steam Dryer Configuration Parameters

<b>Steam Dryer Configuration Parameter</b>	<b>ESBWR Dryer</b>	<b>ABWR Dryer</b>
Number of Banks	6	6
Active height (flow area) for vane modules	1829 mm (65.6 m <sup>2</sup> )	1829 mm (56.6 m <sup>2</sup> )
Approximate weight	60,000 Kg	50,000 Kg
Outside diameter of upper support ring	6919.5 mm	6630 mm
Overall height	5699.5 mm	5695 mm
Length of skirt	2735.5 mm	2731 mm
Skirt thickness	9 mm	7 mm
Cover plate thickness	25.4 mm	16 mm
Hood thickness	25.4 mm (outer bank) 12.7 mm (inner banks)	16 mm (outer bank) 8 mm (inner banks)
Upper support ring cross-section	89 x 242 mm	89 x 242 mm
Average steamline flow velocity	49.7 m/s	42.7 m/s

Table 3L-2 Specific Steam Dryer Load Definition Legend	
Normal (N)	Normal and/or abnormal loads associated with the system operating conditions, including thermal loads, depending on acceptance criteria. These include deadweight, static differential pressure, and fluctuating pressure loads.
TSV	Turbine stop valve closure induced loads in the main steam piping and components integral to or mounted thereon. For the dryer, these include acoustic and flow impact loads. Separate load cases will be evaluated for load components that are separated in time (e.g., acoustic impact and flow impact).
LOCA8	Acoustic impact loads on the dryer due to a postulated steamline break. Separate load cases will be evaluated for load components that are separated in time (e.g., acoustic impact and level swell impact).
LOCA9	Level swell impact loads on the dryer due to a postulated steamline break. Separate load cases will be evaluated for load components that are separated in time (e.g., acoustic impact and level swell impact).

Table 3L-3  
Typical Vibration Sensors

<b>Vibration sensor type</b>	<b>Typical sensor model</b>
Strain gauge	Kyowa Model KHC-10-120-G9
Accelerometer	Vibro-meter Model CA901
Dynamic pressure transducer	Vibro-meter Model CP104 and/or Model CP211

Table 3L-4  
Typical Sensor Locations and Types

<b>Equipment Item</b>	<b>Location on Equipment</b>	<b>Sensor Type</b>	<b>Location Basis</b>
Steam Dryer Support Ring	On top of dryer support	Accelerometer (Acceleration Mode)	Past experience of dryer rocking.
Steam Dryer Skirt	At bottom of dryer	Accelerometer (Displacement Mode)	Modal analysis.
Steam Dryer Hood	At edge of dryer bank hood and end plate.	Strain Gage Pressure Transducer	Past experience of cracks at weld & to obtain forcing function data if problem occurs
Steam Dryer Drain Channel	At top & bottom, side edge of dryer channels.	Strain Gage	Modal analysis. Past experience of cracks at weld.
Steam Dryer Skirt	At top & bottom of dryer skirt.	Strain Gage Pressure Transducer	Modal analysis & to obtain forcing function data if problem occurs
CR Guide Tube	On the outside diameter of the CR guide tube at the midpoint of the guide tube length on a line intersecting the vessel centerline and the guide tube centerline & at a location rotated 90° around the guide tube.	Strain Gage	Modal analysis.
ICM Housing	On the inside diameter of the 90° & 180° vessel azimuth side of the ICM housing at a point 50 mm above the weld between the housing and the vessel bottom head stub tube.	Strain Gage	Modal analysis.
Shroud	On the outside diameter	Strain Gage	Modal analysis.
Top Guide	On the outside diameter of the top guide mounted to measure tangential & radial relative displacements between top guide and vessel.	Linear Variable Differential Transformer (LVDT)	Past experience to measure shroud motion.
Vessel Dome Region	On steam dryer FIV instrument post.	Pressure Transducer	To obtain forcing function data if problem occurs.
Vessel Annulus	On the vertical FIV mounting bar in the annulus between the shroud and vessel walls.	Pressure Transducer	To obtain forcing function data if problem occurs.

Table 3L-5  
Applicable Data Reduction Method for Comparison to Criteria

<b>Component</b>	<b>Sensor Type</b>	<b>Applicable Data Reduction Method</b>		<b>Frequency Bandwidth (Hz)</b>
CR Guide Tubes	Strain Gages	III	Spectrum	0-200
ICM Guide Tubes	Strain Gages	III	Spectrum	0-200
ICM Housings	Strain Gages	I	Time History	0-200
Shroud	Strain Gages	I	Time History	0-100
Steam Dryer Skirt	Strain Gages	I	Time History	0-100
Steam Dryer Drain Channels	Strain Gauges	II	Time History	0-100, 100-200
Steam Dryer Hoods	Strain Gages	II	Time History	0-100, 100-200
Steam Dryer Support Ring	Accelerometer	Impact	Time History	0-1600 0-80, 80-200
Top Guide	Displacement	I	Time History	0-100
Vessel Annulus	Pressure sensors	I	Time History	0-200

Table 3L-6  
Parameters Used in Spectrum Generation

<b>Parameter</b>	<b>Value</b>
Bandwidth	0-200 Hz
Time length	3 minutes
No. of Fourier Lines	400
Resolution	0.5 Hz
Window	Flat Top
No. of averages	90
Overlap	0%
Noise reduction	None
Average Type	Peak-hold
P-P Value	= RMS x 6

Table 3L-7  
Data Evaluation Methods to be Used for Each Component

<b>Internal Component</b>	<b>Data Evaluation Method Used</b>
In-Core Guide Tubes	III
In-Core Housings	I
Control Rod Drive Guide Tubes	III
Shroud and Chimney	I
Steam Dryer	I & II

**Figure 3L-1**  
**Chimney and Partition Assembly**

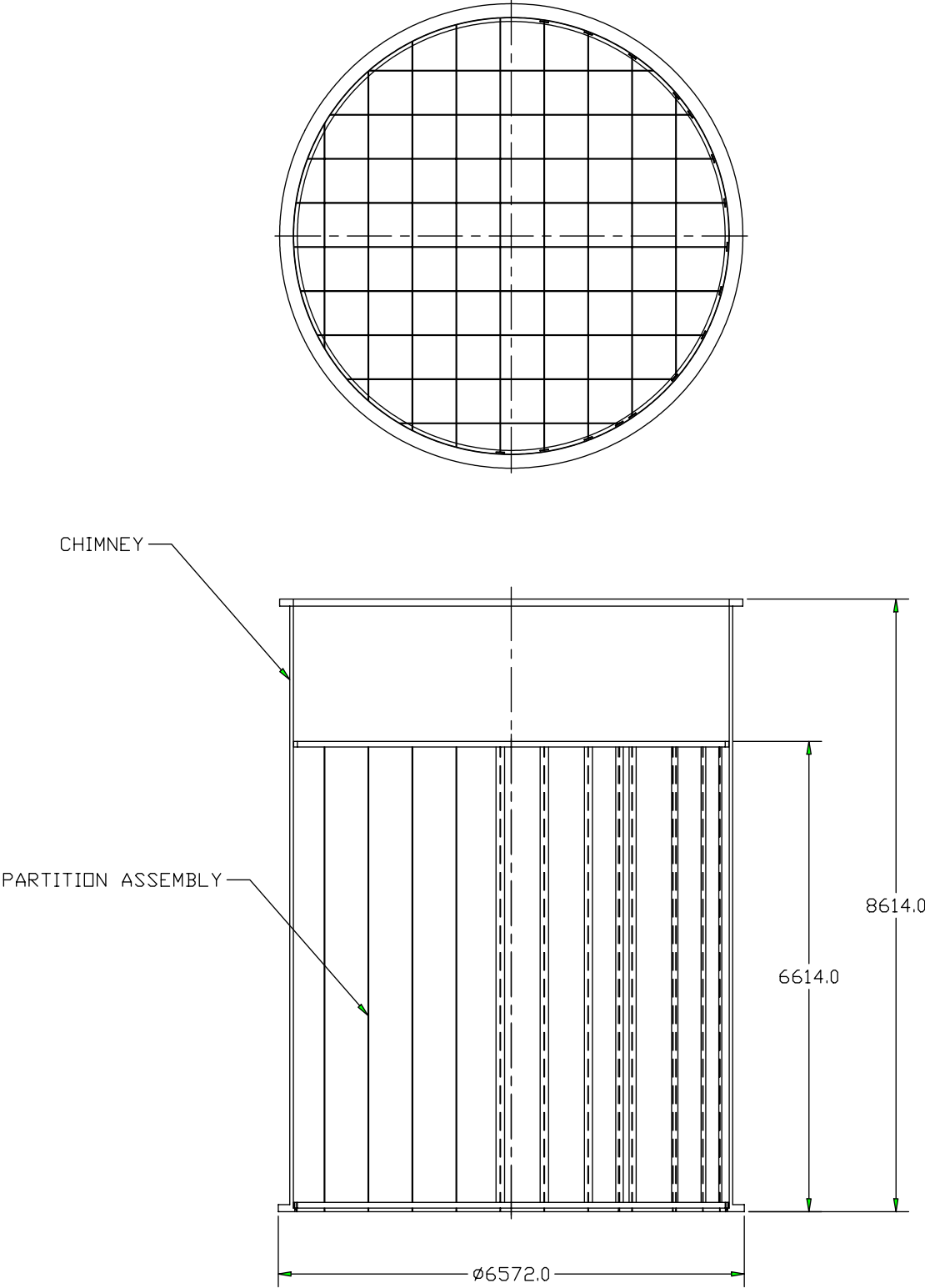




**Figure 3L-2**  
**ESBWR Steam Dryer Assembly**

